Structural Eng./Earthquake Eng., JSCE, Vol. 23, No. 1, 125s-134s, 2006 April
(Translated from a paper which originally appeared on Journal of Earthquake Engineering., JSCE, Vol. 27, 2003. 12)

INFLUENCE OF FAULT MECHANISM, DEPTH, AND REGION ON STRESS DROPS OF SMALL AND MODERATE EARTHQUAKES IN JAPAN

Toshimi SATOH

Member of JSCE, Senior Researcher, Ohsaki Research Institute, Inc.
(Fukoku Seimei Bldg. 2-2-2, Uchisaiwai-cho, Chiyoda-ku, Tokyo, 100-0011, Japan)
E-mail:toshimi@ohsaki.co.jp

Stress drops of 168 earthquakes (focal depth $\leqq$ 60 km, $4.4 \leqq M_W \leqq 6.9$) are estimated by a generalized-inverse method using strong motion records in Japan. Stress drops of crustal earthquakes are dependent of focal depths. Stress drops of reverse-faulting earthquakes are two times greater than those of strike-slip faulting earthquakes and stress drops of strike-slip faulting earthquakes are two times greater than those of normal-faulting earthquakes. These results are consistent with the crustal strength expected from a frictional law. Stress drops of intraplate earthquakes have more variation than those of interplate earthquakes, but are two times greater than those of interplate earthquakes on average.

Key Words: *stress drop, fault mechanism, crustal earthquake, interplate earthquake, intraplate earthquake*

1. INTRODUCTION

It is important for strong motion predictions and simulations using fault models to reasonably determine inner fault parameters for slip heterogeneity as well as outer fault parameters defining the seismic moment and fault area. For example, the strong pulses with a period of about one second observed in the near-field strong motion records during the 1995 Hyogo-ken Nanbu earthquake (M_W6.9) were generated due to asperities within the faults as well as the deep ground structure[1),2)]. Irikura and Miyake[3)] showed how to determine the inner and outer fault parameters of future crustal earthquakes and called their method as the recipe. In the recipe, stress drops on asperities are independent of the style-of-faulting such as reverse, normal, and strike-slip faulting, and independent of the depth of asperities. However, the necessity of depth dependence of stress drops on asperities was pointed out by Irikura *et al.*[4)] through the simulation of strong motion records of the 1995 Hyogo-ken Nanbu earthquake. Recently Dan *et al.*[5)] have shown depth dependency of stress drops on asperities using existing variable-slip rapture models of about 10 large crustal earthquakes in California. However, the stress drops on asperities are estimated by extrapolating from variable-slip rapture models inverted using long period records. Therefore it is necessary to directly estimate stress drops on asperities using broadband strong motion records. Although such problems should be improved, the recipe for crustal earthquakes was applied to several earthquakes and the validity was shown [e.g.,6)] by the comparison between synthetics and empirical attenuation relations.

On the other hand, the recipe for interplate and intraplate earthquakes is now developing. For example, in order to reproduce the seismic intensity distribution and observed strong motion records during the 1978 Miyagiken-oki earthquake of M_W7.6 (an interplate earthquake), stress drops on asperities are set to be greater values than the average for crustal earthquakes and be different values for two asperities[6)]. For intermediate and large intraplate earthquakes, Morikawa *et al.*[7)] estimated source models of several earthquakes in Japan through broadband strong motion simulations using the empirical Green's function method and pointed out that stress drops on asperities of intraplate earthquakes are greater than those crustal and interplate earthquakes. By the same forward modeling technique, Asano *et al.*[8)] showed the depth dependency of stress drops on asperities for shallow intraplate earthquakes. However, a general method to determine stress drops on asperities for future interplate

and intraplate has not been established yet.

Although it is very important to estimate source models by the forward modeling, the number of large earthquakes whose source models with asperities can be inverted is limited. For intermediate and small earthquakes in Japan, stress drops were estimated from broadband strong motion records using a generalized-inverse method by Satoh and Tatsumi[9]. They[9] estimated stress drops of nearly 100 earthquakes in Japan and proposed empirical relations between stress drops and focal depths for crustal earthquakes, though they do not classify crustal earthquakes according to style-of-faultings. In addition, they showed no dependency of stress drops on focal depths for shallow subduction-zone earthquakes, though they do not classify subduction-zone earthquakes into interplate and intraplate earthquakes. Dan *et al.*[5] also proposed empirical relations between stress drops and focal depths according to earthquake types using stress drops extrapolated from existing variable-slip rupture models and those estimated from broadband strong motions records by several researchers. However, some stress drops Dan *et al.*[5] used are estimated by not correcting site-response or estimated from source spectra of average + standard deviation.

In this study, firstly I directly estimate stress drops of 168 earthquakes by the generalized-inverse method[10),11)] using broadband strong motion records in Japan. In order to estimate stress drops more reliably, I select rock and hard soil stations and consider the difference of attenuation around the volcanic front in the northeastern Japan[e.g.,12),13)]. Then I examine the influence of fault mechanism, depth, and region of the stress drops. To examine the influence of fault mechanism, earthquakes are classified into crustal, interplate and intraplate earthquakes according to earthquake types. The crustal earthquakes are classified into reverse, normal, strike-slip, and oblique-slip faultings according to style-of-faultings.

2. DATA

Data are selected on the following conditions from the horizontal components of the acceleration records observed at the ground of K-NET[14)] and KiK-net[15)] strong motion stations from May, 1996 to June, 2002.

1) Earthquakes with focal depth $\leqq$60 km. Subduction-zone earthquakes with $5.0 \leqq M_J \leqq 6.9$ ($4.9 \leqq M_W \leqq 6.7$) and crustal earthquakes with $4.5 \leqq M_J \leqq 6.5$ ($4.4 \leqq M_W \leqq 6.4$). Here M_J is the Japan Meteorological Agency magnitude.

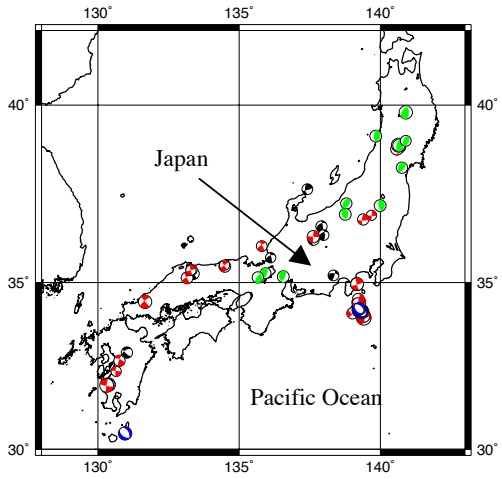

Fig.1 Epicenters and mechanisms of crustal earthquakes. Green, blue, red, and black denote reverse, normal, strike-slip, and oblique-slip earthquakes.

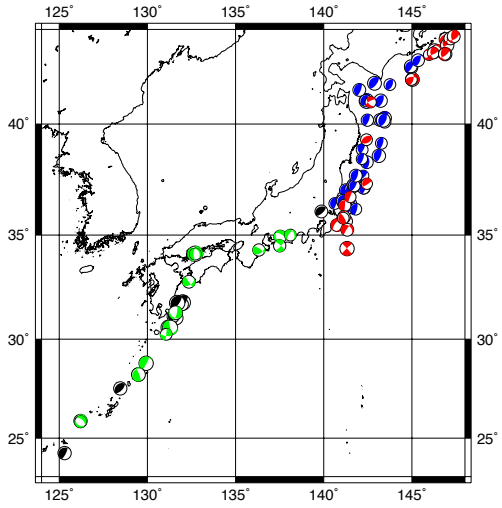

Fig.2 Epicenters and mechanisms of subduction-zone earthquakes. Blue and black denote interplate earthquakes on the Pacific plate and Philippine Sea plate, respectively. Red and green denote intraplate earthquakes within the Pacific plate and Philippine Sea plate, respectively.

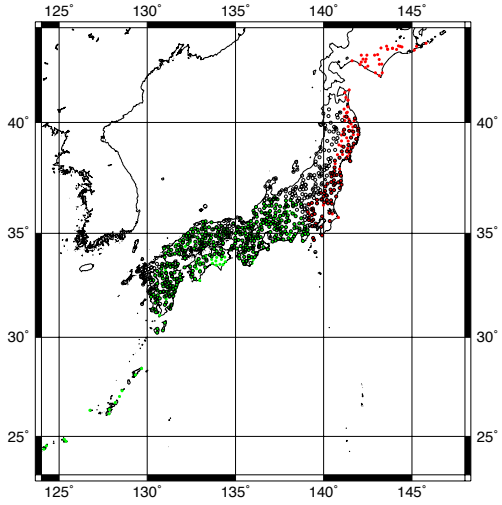

Fig.3 Locations of observation stations. Black circles denotes stations where crustal earthquakes are observed. Red and green denote stations where subduction-zone earthquakes associated with the Pacific plate and the Philippine Sea plate are observed, respectively.

Table1 Number of earthquakes

Crustal earthquake				Interplate earthquake		Intraplate earthquake	
Reverse	Normal	Strike	Oblique	Pacific plate	Philippine Sea plate	Pacific plate	Philippine Sea plate
12	9	36	25	39	10	22	15

2) Records with hypocentral distance $X \leqq 200$ km and triggered at more than three stations per earthquake.
3) Rock or hard soil sites classified into class I on the definition by Japan Road Association[16] using S-wave logging results at observation stations[14),15)]. This selection is used to avoid the contamination of surface waves and the influence of soil nonlinearity.
4) Earthquakes whose focal mechanisms are estimated by F-net[17].
5) Fourier spectra for S-wave windows with duration of 15 seconds are reliable in the frequency range 0.2 to 20 Hz.

The selected data are classified into four subsets, that is, data for subduction-zone earthquakes in the eastern Japan, subduction-zone earthquakes in the western Japan, crustal earthquakes in the eastern Japan, and crustal earthquakes in the western Japan. The eastern and western Japan is divided by the Itoigawa-Shizuoka Tectonic Line, central Japan. Subduction-zone earthquakes in the eastern and western Japan are occurred on and within the Pacific plate and the Philippine Sea plate, respectively. Epicenters of crustal and subduction-zone earthquakes are shown with the focal mechanisms estimated by F-net[17] in **Fig.1** and **Fig.2**, respectively. The hypocenters estimated by the Japan Meteorological Agency are used in this study, The classification by the earthquake types and the style-of-faultings are done based on the focal mechanisms and the focal depths by comparing with the depth distribution of the plates[18),19)]. The subduction-zone earthquakes are classified into interplate and intraplate earthquakes.

Locations of observation stations are shown in **Fig.3**. Stations in the east of the volcanic front are used for subduction-zone earthquakes in the eastern Japan. All stations in the east and west of volcanic front are used for crustal earthquakes. Because the low-Q area (high-attenuation area) extends continuously along the volcanic front in the upper mantle at a depth of 40 km and low-Q area appears only below volcanoes in the crust in the northeastern Japan[13] and so crustal earthquakes tend to be not affected by the low-Q area very much as shown by circular distributions of seismic intensity[12]. All data are about 10,000 waves of 168 earthquakes observed in the total 822 observation stations. The number of earthquakes is listed in **Table 1**.

3. METHOD

(1) Generalized-inverse method[10),11)]

Observed acceleration Fourier spectrum $A_{ij}(f)$ can be written as the product of a source spectrum $S_i(f)$, an attenuation spectrum $P(f)$ and a site-response spectrum $G_j(f)$,

$$A_{ij}(f) = S_i(f) \cdot P(f) \cdot G_j(f) , \qquad (1)$$

where the subscripts i and j refer to the earthquake and the site, respectively. The generalized-inverse method minimizes the error spectrum $ERR(f)$ by the least square method[11].

$$ERR(f) = \sqrt{\frac{1}{\sum_{i=1}^{I}\sum_{j=1}^{J}\delta_{ij}}} \times$$

$$\sqrt{\sum_{i=1}^{I}\sum_{j=1}^{J}\delta_{ij}\left\{\log_{10} A_{ij}(f) - S_i(f) - P(f) - G_j(f)\right\}^2} \qquad (2)$$

Here δ_{ij} =1 for the observed records, and δ_{ij} = 0 otherwise. IWT009 (Daito) of a K-NET station is selected as a reference station, because Satoh and Tatsumi[9] pointed out the site effects are free in the frequency range of less than 4 Hz.

An attenuation spectrum $P(f)$ is modeled by geometrical spreading factor and the anelastic attenuation function with the quality factor $Q(f)$.

$$P(f) = \frac{1}{X}\exp\left(\frac{-\pi f X}{Q(f)\beta}\right) , \qquad (3)$$

where β is the medium's average S-wave velocity and assumed to be 3.4 km/s and 4 km/s for crustal and subduction-zone earthquakes, respectively. It is pointed out that attenuation characteristics of records for crustal earthquakes can be explained better by assuming geometry spreading of $1/X^{1/2}$ for distances > 50 to 150 km than $1/X$ for over all distances[e.g.,20)]. This is attributable to mid-to-deep crustal reflections and Lg waves [e.g.,20)]. Therefore, for crustal earthquakes data, the transition distance Xr of the two-segment geometry spreading is estimated by a grid search technique[9] to minimize $ERR(f)$. The grid increment is 20 km and the search range is 40 to 160 km.

(2) Stress drop estimation

The source spectrum $S(f)$ deconvolved by the generalized-inverse method can be modeled by ω^{-2} model model[21),22)] as

$$S(f) = \frac{R_{\theta\phi} F_S P_{RTITN}}{4\pi\rho\beta^3} \sqrt{\frac{\rho\beta}{\rho_z\beta_z}} \frac{(2\pi f)^2 M_0}{1+\left(\frac{f}{f_0}\right)^2}, \quad (4)$$

where ρ and β are the density and S-wave velocity at the source, β_z and ρ_z are the density and S-wave velocity at the reference site IWT009. I use ρ=2.7 g/cm^3, β=3.4 km/s for crustal earthquakes, ρ=3.0 g/cm^3, β=4.0 km/s for subduction-zone earthquakes. Based on the logging results at the reference station and the nearby stations, β_z and ρ_z are taken[9)] to be 2.85 km/s and 2.65 g/cm^3. $R_{\theta\phi}$ is a radiation coefficient and to be equal to 0.55 of the logarithmically averaged radiation patterns for S-waves[23)]. F_s is the free surface amplification (F_s=2). P_{RTITN} is the reduction factor that accounts for the partitioning of energy into two horizontal components and is taken to be unity because a vector of two horizontal spectra is used as source spectrum.

A corner frequency f_0 is estimated[24)] to minimize $J(f_0)$ using revised quasi-Newton method.

$$J(f_0) = \int_{fs}^{fe} (O(f) - M(f))^2 df, \quad (5)$$

where

$$O(f) = \frac{S(f)}{\frac{R_{\theta\phi} F_S P_{RTITN}}{4\pi\rho\beta^3} \sqrt{\frac{\rho\beta}{\rho_z\beta_z}}}, \quad (6)$$

and

$$M(f) = \frac{(2\pi f)^2 M_0}{1+\left(\frac{f}{f_0}\right)^2}. \quad (7)$$

Here the value of a seismic moment M_0 is taken from estimates by F-net[17)]. The minimum frequency fs is 0.2 Hz and maximum frequency fe is 4 Hz because there is no site-response in this frequency range at IWT009[9)].

Brune's[21)] stress drop $\Delta\sigma$ is calculated by

$$\Delta\sigma = M_0 \{ f_0/(4.9\times10^6 \beta) \}^3, \quad (8)$$

The initial value of f_0 is calculated from the equation (8) using $\Delta\sigma$=50 bars, which is average stress drop of earthquakes in Japan[25)]. The Brune's stress drop is changed into the equivalent Madariaga's[26)] stress drop by multiplied 1/0.72 to the Brune's stress drop in order to match with the definition of stress drops on asperities[4)]. Here rupture velocity is assumed to be 0.72 times of S-wave velocity[27)].

In addition, the flat level of acceleration source spectrum A is calculated[21),28)] from

$$A = 4\pi^2 f_0^2 M_0. \quad (9)$$

Then the difference of the relation between M_0 and A according to earthquake types is examined, because the relation between M_0 and A is important to set stress drops on asperities[3),28)].

4. RESULTS

(1) Q value

Fig.4(a) shows Q^{-1} estimated from records of subduction-zone earthquakes by the generalized-inverse method. The least square lines fitted in the frequency range 0.5 to 10 Hz are Q=154$f^{0.91}$ and Q=199$f^{0.41}$ for the eastern and western subduction-zone earthquakes, respectively. The Q^{-1} value in the eastern Japan is greater in the low frequency range and smaller in the high frequency range than the Q^{-1} values in the western Japan. This tendency is con-

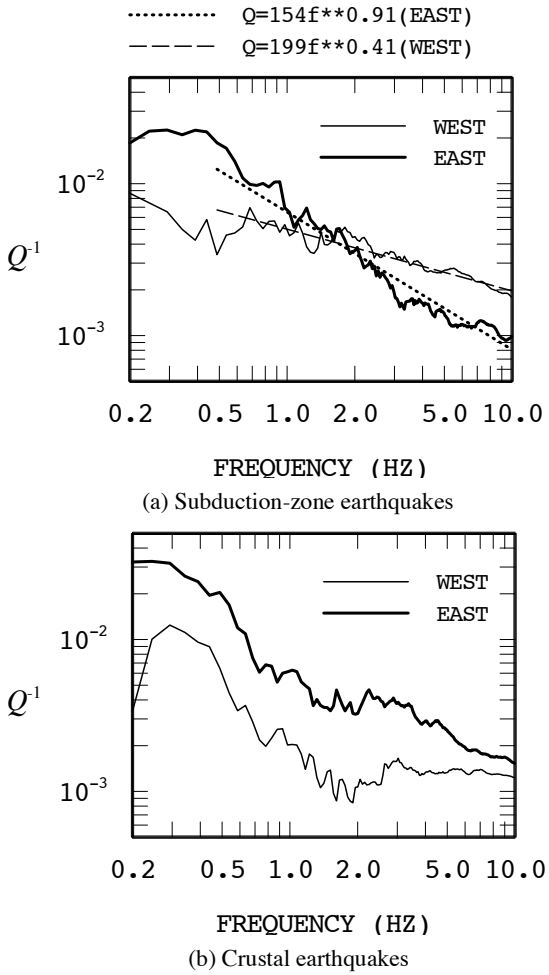

Fig.4 Estimated Q^{-1} values and the least square fitting lines.

sistent with the distribution of Q^{-1} values in the depth range 0 to 30 km estimated by Nakamura and Uetake[29].

Fig.4(b) shows Q^{-1} estimated from the records of crustal earthquakes. The transition distance Xr is estimated to be 80 km for both the eastern and western Japan. The value of Xr = 80 km in Japan is the same as that estimated by Satoh and Tatsumi[9] and consistent with that estimated from records in the United States. The Q^{-1} in the western Japan is especially small with 10^{-3} in the frequency range 1 to 2 Hz. This small value is similar to that in the depth range 0 to 30 km in the wide region of western Japan estimated by Nakamura and Uetake[29].

(2) Source spectrum and estimated stress drops

Fig.5 compares between the acceleration source spectra deconvolved by the generalized-inverse method and the fitted ω^{-2} model for an interplate earthquake (M_W5.1) occurred on the Pacific plate. The deconvolved source spectrum shape is well described by the ω^{-2} model.

The estimated values of stress drops are shown by the size of the circles in **Fig.6**. On average, stress drops of crustal earthquakes are smaller than those of interplate and intraplate earthquakes. The regional variation of stress drops of interplate earthquakes is smaller than that of intraplate earthquakes. In the region where stress drops of interplate earthquakes are relatively large, stress drops of intraplate earthquakes also tend to be large. In addition, stress drops of most of intraplate earthquakes within the Philippine Sea plate are large as shown later in detail. For example the stress drop of the intraplate earthquake within the Philippine Sea plate on March 24, 2001, called the 2001 Geiyo earthquake (M_W6.7), is estimated to be 84 MPa. The stress drop of the aftershock (M_W5.1) on March 26 is estimated to be

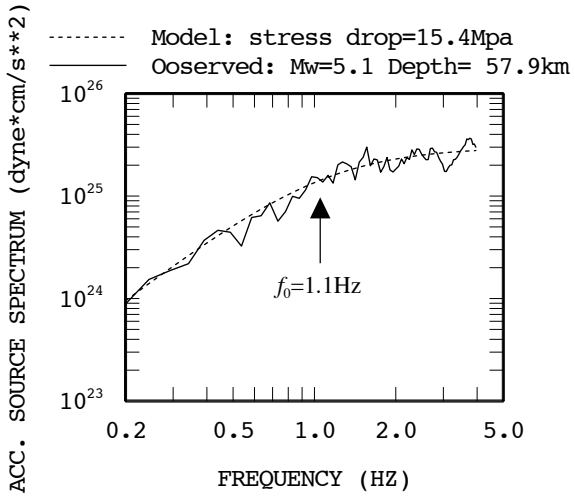

Fig.5 Comparison between the acceleration source spectra estimated by the generalized-inverse method and the fitted ω^{-2} model for an interplate earthquake (*Mw*5.1).

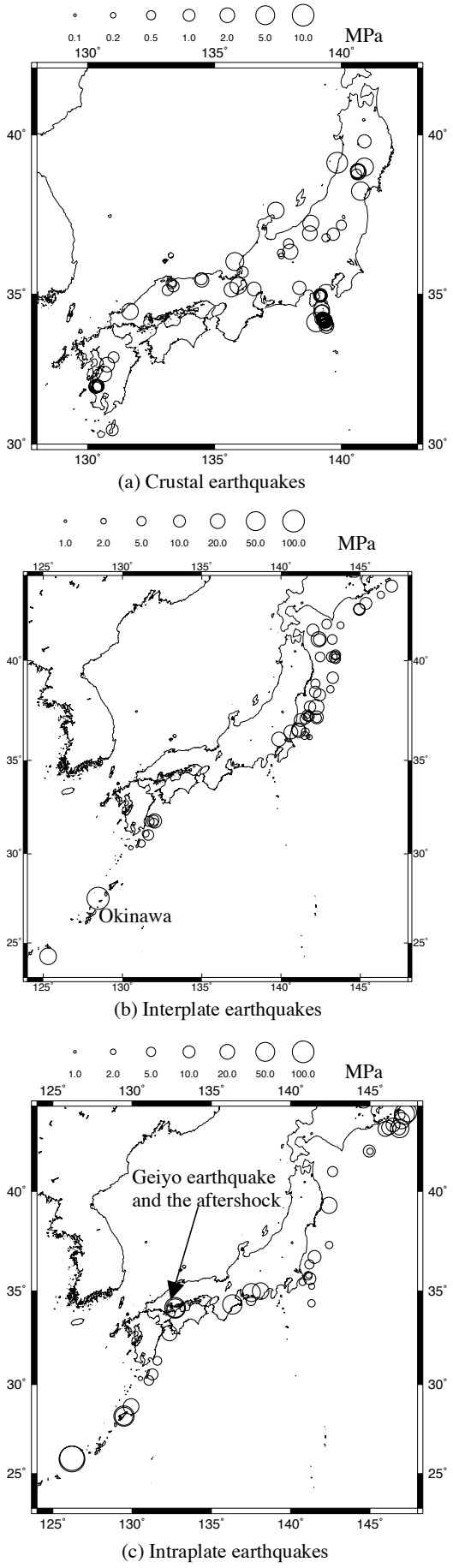

Fig.6 Estimated stress drops. The size of circles depends of the stress drop values.

49 MPa. On the other hand, stress drops of strike-slip intraplate earthquakes (See **Fig.2** and **Fig.6**) tend to be small among all intraplate earthquakes.

(3) Influence of mechanism, depth and region on stress drops

In **Fig.7** stress drops of crustal earthquakes according to style-of-faultings are plotted against focal depth, revealing the increase of stress drops with depth. The stress drops $\Delta\sigma$ in MPa are represented as a function of depth D in km by

$$\Delta\sigma = a+b\times D, \qquad (10)$$

where a and b are regression coefficients. The form of this equation is based on the Byerlee 's[30] frictional law in the brittle potion of the crust and is also known as Coulomb-Mohr law as

$$\tau = \tau_0+\mu\times\sigma_n^{eff} = \tau_0+\mu\times(\sigma_n-P)\,, \qquad (11)$$

where τ is the shear strength, μ is the coefficient of friction, σ_n^{eff} is the effective normal stress, σ_n is the normal stress, P is the pore pressure, and τ_0 is the cohesive strength. If P is assumed to be hydrostatic and μ is assumed to be 0.75 in the frictional law, the crustal strength is expected to increase linearly with depth and the crustal strength of the compressional tectonic regime is about 4 times larger than that of the extensional tectonic regimes[31),32)]. The stress regime giving rise to strike-slip earthquakes is within the bounds of compressional and extensional regimes[31),32)].

The regression lines obtained in this study shown in **Fig.7** are as follows.

$$\Delta\sigma = 0.337+0.103D \quad \sigma=1.06 \text{ (strike-slip)} \qquad (12)$$
$$\Delta\sigma = 1.204+0.327D \quad \sigma=1.59 \text{ (reverse)} \qquad (13)$$
$$\Delta\sigma = 0.380+0.029D \quad \sigma=0.19 \text{ (normal)} \qquad (14)$$
$$\Delta\sigma = 0.554+0.044D \quad \sigma=0.56 \text{ (oblique-slip)} \qquad (15)$$

Here σ is one standard deviation. Data with a depth of 0 km are excluded for the regression analyses because 0 km is not acceptable in a physical sense. The regression lines indicate that stress drops of reverse earthquakes are the largest and stress drops of normal earthquakes are the smallest. At a depth of about 15 km, which is equal to the center of the data, Stress drops of reverse earthquakes are two times greater than those of strike-slip earthquakes and stress drops of strike-slip earthquakes are two times greater than those of normal earthquakes. These results are consistent with the expectations from the frictional law mentioned above. The similar results were shown using peak ground accelera-

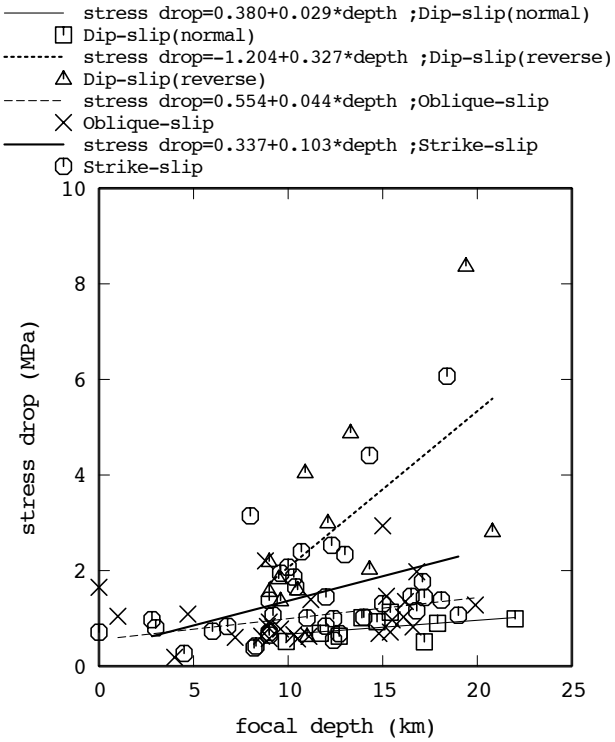

Fig.7 Relationship between stress drops between focal depths for crustal earthquakes according to style-of-faultings.

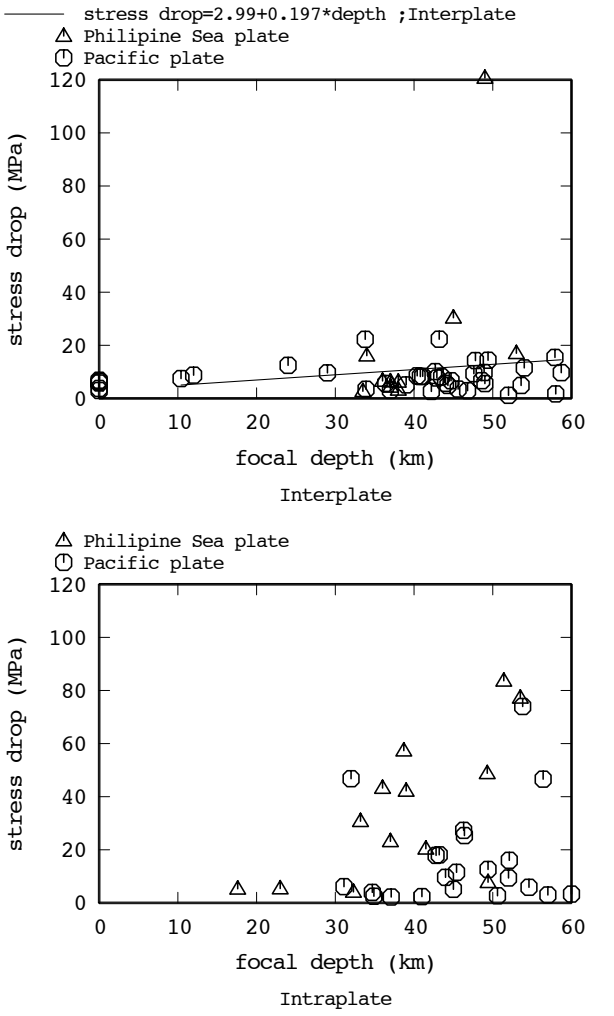

Fig.8 Relationship between stress drops between focal depths for interplate and intraplate earthquakes.

tions and peak ground velocities of near-field strong motion records for crustal earthquakes in the United states by McGarr[32]. However, McGarr[32] did not correct site-responses at observed stations and anelastic attenuation associated with Q values from observed records. In my paper, both effects are corrected from observed records by using the generalized-inverse method. In some previous empirical attenuation relations[33),34),35)] of peak ground accelerations and response spectra of strong motions for crustal earthquakes outside Japan the style-of-faulting has been considered, but the depth dependence has not been considered. The result suggests that the style-of-faulting and depth would be appropriate as parameters for empirical attenuation relations for crustal earthquakes in Japan.

In **Fig.8** stress drops of interplate and intraplate earthquakes are plotted against focal depth. Two intraplate earthquakes around Okinawa in southwestern islands with stress drops of greater than 200 MPa are not shown in **Fig.8**. Stress drops of interplate earthquakes are less than about 30 MPa except for an earthquake occurred near Okinawa. No clear depth dependencies of stress drops for interplate earthquakes can not be seen, though Ruff[36)] showed that the dynamic stress drops of interplate earthquakes at Sanriku in the northeastern Japan and in Mexico increase with depth.

Stress drops of intraplate earthquakes have a large variation compared with those of interplate earthquakes. For intraplate earthquakes, the maximum bound of stress drops increases with depth and stress drops of about 1/3 earthquakes are beyond 30 MPa. All interplate earthquakes are thrust earthquakes, while intraplate earthquakes include several different style-of-faultings, such as down-dip-compression, down-dip-extension, reverse, normal, and strike-slip. This may be a cause of the difference in the variation of stress drops for interplate and intraplate earthquakes. Stress drops of intraplate earthquakes seems to be depth-dependent within the Philippine Sea plate but not the Pacific plate. The depth dependency is probably different in regions associated with rheology.

The geometrical average of stress drops for interplate and intraplate earthquakes are 7 MPa and 15 MPa, respectively, which yields two times difference. The geometrical average of stress drops for interplate earthquakes on the Pacific plate and Philippine Sea plate are similar, that is, 7 MPa and 9 MPa, respectively. On the other hand, The geometrical average of stress drops for intraplate earthquakes in the eastern and western Japan are 10 MPa and 31 MPa, respectively, which yields three times difference.

(4) Relation between flat level of acceleration source spectra and seismic moment

Fig.9 shows relation between flat level of acceleration source spectra A and seismic moment M_0. Data in this figure are from this study and Dan *et al.*[28)] who estimated A from variables-slip rupture models. Dashed lines are empirical relations of Dan

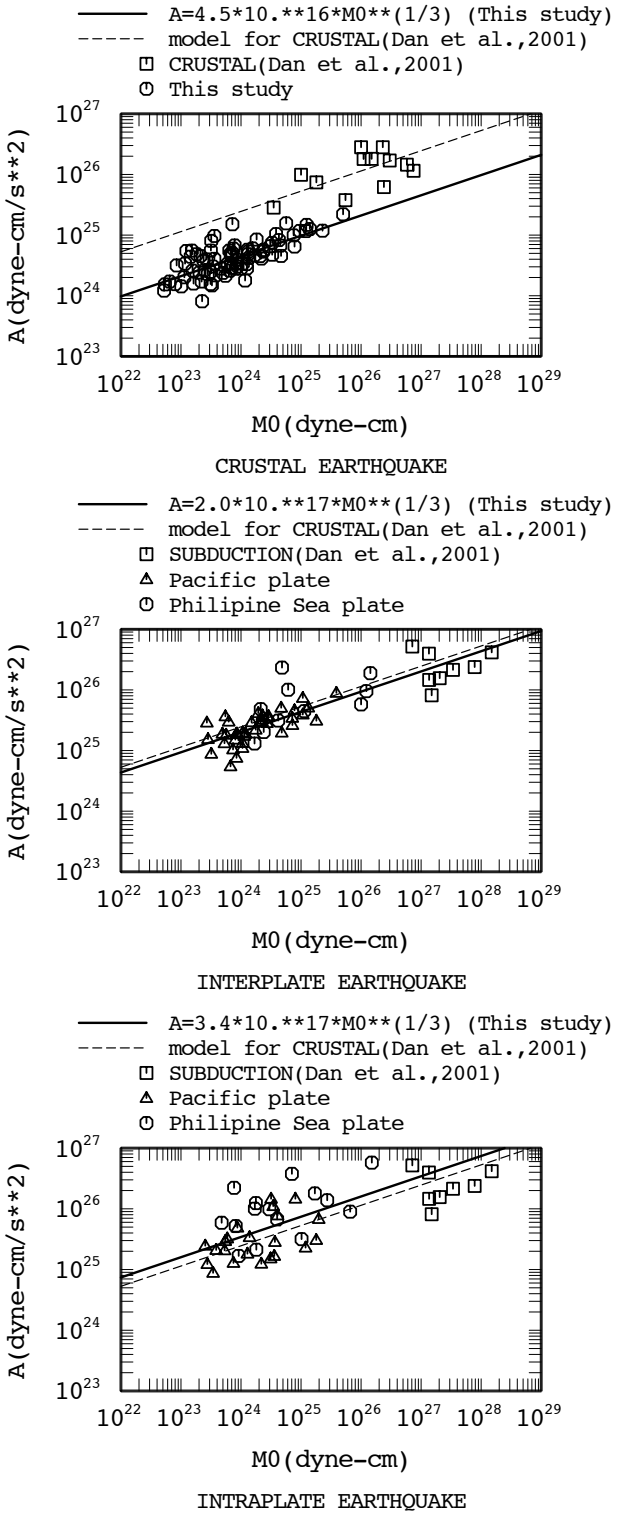

Fig.9 Relationship between flat level of acceleration source spectra A and seismic moment M_0.

et al. for crustal earthquakes. Solid lines are empirical relations fitting the data in this study. All the empirical lines are obtained assuming $M_0^{1/3}$ scaling for *A*. Empirical relations obtained in this study are

$$A=4.5\times10^{16}\times M_0^{1/3} \text{ (crustal earthquakes)} \quad (16)$$
$$A=2.0\times10^{17}\times M_0^{1/3} \text{ (interplate earthquakes)} \quad (17)$$
$$A=3.4\times10^{17}\times M_0^{1/3} \text{ (intraplate earthquakes).} \quad (18)$$

The *A* of the empirical relation for crustal earthquakes in this study is 1/5 smaller than the Dan *et al*.'s[28] relation. Satoh and Tatsumi[9] showed that the M_0-*A* relation of relatively large crustal earthquakes, that is, the 1995 Hyogo-ken Nanbu earthquake (M_W6.9) and the 2000 Tottori-ken Seibu earthquake (M_W6.6), are reasonably consistent with the Dan *et al*.'s[28] relation, but that *A* of small and moderate earthquakes with $M_0 < 2\times10^{25}$ dyne-cm ($M_W < 6.2$) are smaller than *A* by the Dan *et al*.'s[28] relation. The M_0-*A* relation in this study is consistent with the relation for small and moderate earthquakes by Satoh and Tatsumi[9]. This result means that the $M_0^{1/3}$ scaling inferred for *A* dose not hold true for all sizes of earthquakes. In other words, this result suggests the break of scaling for crustal earthquakes.

On the other hand, the M_0-*A* relation for interplate earthquakes in this study is similar to the data for interplate earthquakes estimated by Dan *et al*.[28] and the Dan *et al*.'s[28] relation for crustal earthquakes. In the M_0-*A* relations, *A* for intraplate earthquakes is 1.5 times greater than *A* for interplate earthquakes. Especially *A* for intraplate earthquakes within the Philippine Sea plate is nearly three times greater than *A* for interplate earthquakes.

5. CONCLUSIONS

Stress drops of 168 earthquakes (focal depth $\leqq$ 60 km, $4.4\leqq M_W\leqq6.9$) are estimated to minimize the residuals between ω^{-2} model and source spectra deconvolved by a generalized-inverse method using K-NET and KiK-net strong motion records in Japan. Using the estimated stress drops, the influence of fault mechanism, depth, and region of the stress drops and flat level of acceleration source spectra *A* are examined. The results are as follows.

1) Stress drops of crustal earthquakes increase with focal depth and so the empirical relations between stress drops and focal depths are proposed according to style-of-faultings. Around the center of the data the stress drops of reverse-faulting earthquakes are two times greater than those of strike-slip faulting earthquakes and the stress drops of strike-slip faulting earthquakes are two times greater than those of normal-faulting earthquakes. These results are consistent with the crustal strength expected from a frictional law.

2) Stress drops of interplate earthquakes are less than about 30 MPa and have no clear depth dependencies. For intraplate earthquakes, the maximum bound of stress drops increases with depth. The stress drops of intraplate earthquakes have a large variation compared with those of interplate earthquakes region. Possible causes of the large variation in stress drops of intraplate earthquakes may be the variation of fault mechanisms.

3) The geometrical average of stress drops for interplate and intraplate earthquakes are 7 MPa and 15 MPa, respectively, which yields two times difference. The geometrical average of stress drops for interplate earthquakes on the Pacific plate and Philippine Sea plate are 7 MPa and 9 MPa, respectively. On the other hand, The geometrical average of stress drops for intraplate earthquakes within the Pacific plate and the Philippine Sea plate are 10 MPa and 31 MPa, respectively, which yields three times difference.

4) The obtained empirical relation between *A* and seismic moment M_0 for interplate earthquakes is consistent with the relation estimated by Dan *et al*.[28] for crustal earthquakes extrapolated from variable-slip rupture models. On the other hand, *A* for intraplate earthquakes is 1.5 times greater than *A* for interplate earthquakes.

5) Stress drops and *A* for small crustal earthquakes are smaller than large crustal earthquakes. The transition M_0 is around 2×10^{25} dyne-cm. This result means that the $M_0^{1/3}$ scaling inferred for *A* dose not hold true for all sizes of earthquakes.

There are several aspects of this study that should be pursued further. In the generalized-inverse analysis, data are classified into 4 subsets and include relatively far stations from sources because of limitations of data and the method. However, in order to estimate source parameters, that is, stress drops and flat level of acceleration source spectra *A* more accurately, it is better to use only near-fault records and consider the more precise regional differences of *Q* values. In addition, the depth-dependency of stress drops of intraplate earthquakes should be examined by including deeper (> 60 km) earthquakes since deeper earthquakes, such as 1994 Kushiro-oki eathquake[7] (M_W7.6) and the 2003 Miyagiken-oki earthquake[37] (M_W7.0) have been reported to have large stress drops and *A*.

ACKNOWLEDGMENT: I used strong motion records and S-wave logging results of K-NET and KiK-net and focal mechanisms of F-net deployed by

National Research Institute for Earth Science and Disaster Prevention, Japan. I use moment magnitude M_W estimated by Harvard University and F-net for earthquakes before and after 1997, respectively. I also use the earthquake hypocenter information estimated by the Japan Meteorological Agency. GMT by Wessel and Smith[38] was used for making several figures.

REFERENCES

1) Matsushima, S. and Kawase, H.: Multiple asperity model of the Hyogo-ken Nanbu earthquake of 1995 and strong motion simulation in Kobe, *J. Struct. Constr. Eng., Architectual Institute of Japan*, No.534, pp.33-40, 2000 (in Japanese with English abstract).
2) Kawase, H.: The cause of the damage belt in Kobe: The basin-edge effect, Constructive interference of the direct S-wave with the basin-induced diffracted/Rayleigh waves, *Seism. Res. Lett.*, Vol.67, pp. 25-34, 1996.
3) Irikura, K. and Miyake, H.: Prediction of strong ground motions for scenario earthquake *Journal of Geography,* Vol.110, pp.849-875, 2001 (in Japanese with English abstract).
4) Irikura, K., Miyake, H., Iwata, T., Kamae, K. and Kawabe, H.: Revised recipe for predicting strong ground motion and its validation, *Proc. 11th Japan Earthquake Engineering Symp.*, CD-ROM, 109.pdf, 2002 (in Japanese with English abstract).
5) Dan, K., Watanabe, M. and Miyakoshi, J. : Empirical relation of effective stress on asperity to fault type and depth inferred from existing spectrum inversion results and source inversion results, *J. Struct. Constr. Eng., Architectual Institute of Japan*, No.565, pp.55-62, 2003 (in Japanese with English abstract).
6) Ishii, T., Fujiwara, H., Aoi, S., Sato, T., Watanabe, M., Satoh, T., Matsushima, S., Hayakawa, T., Shinohara, H., Iwamoto, K., Nozaki, K. and Senna, S.: Study on hazard maps for inland and subduction earthquakes in Japan, Paper No.1904, *Proc. 13th World Conference on Earthquake Engineering*, 2004.
7) Morikawa, N., Sasatani, M. and Fujiwara, H.: Construction of source models of intra-slab earthquakes using empirical Green's function method, *Proc. 11th Japan Earthquake Engineering Symp.*, CD-ROM, 27.pdf, 2002 (in Japanese with English abstract).
8) Asano, K., Iwata, T. and Irikura, K.: Source characteristics of shallow intraslab earthquakes derived from strong-motion simulations, *Earth Planets Space*, Vol.55, pp.e5-e8, 2003.
9) Satoh, T. and Tatsumi, Y.: Source, path, and site effects for crustal and subduction earthquakes inferred from strong motion records in Japan, *J. Struct. Constr. Eng., Architectural Institute of Japan*, No.556, pp.15-24, 2002 (in Japanese with English abstract).
10) Iwata, T. and Irikura, K.: Source parameters of the 1983 Japan Sea earthquake sequence, *J. Phys. Earth,* Vol.36, pp.155-184, 1988.
11) Dan, K., Miyakoshi, J. and Yashiro, K.: Simple procedure for evaluating earthquake response spectra of large-event motions based on site amplification factors derived from smaller-event records, *J. Struct. Constr. Eng., Architectural Institute of Japan*, No.480, pp.35-46, 1996 (in Japanese with English abstract).
12) Ikami, A.: Attenuation of seismic waves beneath the volcanic front, *Zisin* (*J. Seismol. Soc. Jpn*), Ser. 2, Vol.28, pp.61-73, 1975 (in Japanese with English abstract).
13) Sekine, S., Matsubara, M., Obara, K. and Kasahara, K.: Estimation of site effects and Q structure beneath the Japan Islands derived from NIED Hi-net data, *Abstracts of Japan Earth Planetary Science Joint Meeting*, S069-P006.pdf, 2003.
14) Kinoshita, S.: Kyoshin Net (K-NET), *Seism. Res. Lett.,* Vol.69, pp.309-332, 1998.
15) Aoi, S., Obara, S., Hori, S., Kasahara, K. and Okada Y.: New strong motion observation network: KiK-net, *EOS Trans. Am. Geophys. Union*, Vol.81, F863, 2000.
16) Japan Road Association: *Specification for Highway Bridges, Part V, Earthquake Resistant Design*, 2002 (in Japanese).
17) Fukuyama, E., Ishida, S., Dreger, D.S. and Kawai, H.: Automated seismic moment tensor determination by using on-line broadband seismic waveforms, *Zisin* (*J. Seismol. Soc. Jpn*), Ser.2, Vol.51, pp.149-156, 1998 (in Japanese with English abstract).
18) Hasegawa, A., Umino, N. and Takagi, A.: Seismicity in the northern Japan arc and seismicity patterns before large earthquakes, *Earthq. Pred. Res.*, Vol.3, pp.607-626, 1985.
19) Yamazaki, F. and Ooida, T.: Configuration of subducted Philippine Sea plate beneath the Chubu district, central Japan, *Zisin* (*J. Seismol. Soc. Jpn*), Ser.2, Vol.38, pp.193-203, 1985(in Japanese with English abstract).
20) Boore, D.M. and Atkinson, G.M.: Source spectra for the 1988 Saguenay, Quebec, earthquakes, *Bull. Seism. Soc. Am.*, Vol.82, pp.683-719, 1992.
21) Brune, J.N.: Tectonic stress and the spectra of seismic shear waves from earthquakes, *J. Geophys. Res.*, Vol.75, pp.4997-5009, 1970.
22) Boore, D.M.: Stochastic simulation of high-frequency ground motions based on seismological models of the radiated spectra, *Bull. Seism. Soc. Am.*, Vol.73, pp.1865-1894, 1983.
23) Boore, D.M. and Boatwright, J.: Average body-wave radiation coefficient, *Bull. Seism. Soc. Am.*, Vol.74, pp.1615-1621, 1984.
24) Satoh, T., Kawase, H. and Sato, T.: Statistical spectral model of earthquakes in the eastern Tohoku district, Japan based on the surface and borehole records observed in Sendai, *Bull. Seism. Soc. Am.*, Vol.87, pp.446-462, 1997.

25) Sato, R.: *The Parameter Handbook on Earthquake Faults in Japan*, Kajima Institute Publishing Co., Ltd., 1989.
26) Madariaga, R.: High-frequency radiation from crack (stress drop) models of earthquake faulting, *Geophysical Journal of the Royal Astronomical Society*, Vol.51, No.3, pp.625-651, 1977.
27) Geller, R.J.: Scaling relations for earthquake source parameters and magnitudes, *Bull. Seism. Soc. Am.,* Vol.66, pp.1501-1523, 1972.
28) Dan, K., Watanabe, M., Sato, T. and Ishii, T.: Short-period source spectra inferred from variable-slip rupture models and modeling of earthquake fault for strong motion prediction, *J. Struct. Constr. Eng., Architectural Institute of Japan*, No.545, pp.51-62, 2001 (in Japanese with English abstract).
29) Nakamura, R. and Uetake, T.: Three dimensional attenuation structure and site amplification inversion by using a large quantity of seismic strong motion records in Japan, *Zisin* (*J. Seismol. Soc. Jpn*), Ser.2, Vol.54, pp.475-488, 2002 (in Japanese with English abstract).
30) Byerlee, J.D.: Friction of rocks, *Pure Appl. Geophys.*,Vol.116, pp.615-625, 1978.
31) Brace, W.F. and Kohlstedt, D.L.: Limits on lithospheric stress imposed by laboratory experiments, *J. Geophys. Res.,* Vol.85, pp.6248-6252, 1980.
32) McGarr, A.: Scaling of ground motion parameters, state of stress, and focal depth, *J. Geophys. Res.*, Vol.89, pp.6969-6979, 1984.
33) Abrahamson, N.A. and Silva, W.J.: Empirical response spectral attenuation relations for shallow crustal earthquakes, *Seismo. Res. Lett.*, Vol.68, pp.94-127, 1997.
34) Boore, D.M., Joyner, W.B. and Fumal, T.E.: Equations for estimating horizontal response spectra and peak acceleration from western North American earthquakes: A summary of recent work, *Seismo. Res. Lett.*, Vol.68, pp.128-153, 1997.
35) Spudich, P., Fletcher, J.B., Hellweg, M., Boatwright, J., Sullivan, C., Joyner, W.B., Hanks, T.C., Boore, D.B., McGarr, A., Baker, L.M. and Lindh, A.G.: Sea96-A new predictive relation for earthquake ground motions in extensional tectonic regimes, *Seismo. Res. Lett.*, Vol.68, pp.190-198, 1997.
36) Ruff, L.J.: Dynamic stress drop of recent earthquakes: Variations with subduction zones, *Pure Appl. Geophys.*, Vol.154, pp.409-431, 1999.
37) Satoh, T.: Short-period spectral level of intraplate and interplate earthquakes occurring off Miyagi prefecture, *Journal of Japan Association for Earthquake Engineering*, Vol.4, No.1, pp.1-4, 2004 (in Japanese with English abstract).
38) Wessel, P. and Smith W.H.F.: New, improved version of Generic Mapping Tools released, *EOS*, AGU, 1998.

(Received June 1, 2005)